ELSEVIER

Physica C 300 (1998) 225–238

PHYSICA C

Influence of the doping level on the charge distribution among the inequivalent CuO_2 layers in $Tl_2Ba_2Ca_2Cu_3O_{10-\delta}$: a NMR study

Y.V. Piskunov [a], K.N. Mikhalev [a], Yu.I. Zhdanov [a], A.P. Gerashenko [a], S.V. Verkhovskii [a,*], K.A. Okulova [a], E.Yu. Medvedev [a], A.Yu. Yakubovskii [b], L.D. Shustov [b], P.V. Bellot [c], A. Trokiner [c]

[a] *Institute of Metal Physics, Russian Academy of Sciences, Ural Division, Ekaterinburg, Russian Federation*
[b] *Russian Scientific Center 'Kurchatov Institute', Moscow, Russian Federation*
[c] *Ecole Superieure de Physique et Chimie Industrielles, Paris, France*

Received 26 December 1997

Abstract

^{63}Cu and ^{17}O NMR measurements in the normal and superconducting states of $Tl_2Ba_2Ca_2Cu_3O_{10-\delta}$ with different δ are reported. In the overdoped Tl2223 sample with $T_c = 117$ K ($T_c^{opt} = 123$ K) and $\delta_1 < \delta^{opt}$ different temperature dependencies of the Knight shift ^{17}K are revealed for inequivalent CuO_2 layers. For the inner CuO_2 layer with the square oxygen coordination of Cu the decrease of ^{17}K with temperature is more gradual. In going towards the underdoped Tl2223 with $T_c = 104$ K and $\delta_2 > \delta^{opt}$ the changes of $^{63,17}K$ with temperature are found to be the same for both types of copper layers. The quadrupole coupling constants for copper and oxygen from different CuO_2 layers were obtained. From the variations with doping of the valence contribution to the electric field gradient at copper sites, we estimate both the hole numbers at Cu and oxygen sites and the real concentration of mobile hole carriers n_h in each of inequivalent CuO_2 layers. In the overdoped Tl2223 sample the charge density in the inner layer differs from the one in the outer plane (with five-fold oxygen coordination for Cu). Our results show that the inhomogeneity of the charge distribution disappears in the underdoped regime. The results are compared with calculations of the charge distribution among the CuO_2 planes in multilayered cuprates reported by Haines and Tallon [E.M. Haines, J.L. Tallon, Phys. Rev. B 45 (1992) 3127].

Keywords: ^{63}Cu; ^{17}O NMR; Knight shift; Electric field gradient; $Tl_2Ba_2Ca_2Cu_3O_{10-\delta}$; CuO_2 planes; Distribution of holes

1. Introduction

High-T_c superconducting copper oxides $Tl_2Ba_2Ca_nCu_{n+1}O_{6+2n-\delta}$ have a layered structure which includes perovskite-like CuO_2 planes. The features of electronic excitations in these layers determine superconducting properties of the compound and depend on concentration of holes in the layer. The crystallographically inequivalent CuO_2 planes, in which copper atoms have different coordination with the nearest oxygen atoms, appear at $n = 2$. In the two outer layers of Tl2223, the copper atoms,

* Corresponding author. Institute of Metal Physics, Kovalevskaya str. 18, Ekaterinburg 620219, Russian Federation. Fax: +7-3432-74-52-44; e-mail: verkhovskii@ifm.ural.ru.

0921-4534/98/$19.00
PII S0921-4534(98)00102-6

Cu(1), have the pyramidal nearest environment similar to the oxygen five-fold coordination of Cu in the CuO_2 layers of $YBa_2Cu_3O_7$. For the inner layer positioned between two planes of Ca the Cu(2) atoms have a square-plane coordination with the four nearest oxygen atoms.

In cuprates, superconducting transition temperature T_c reaches a maximum near the hole concentration $n_h^{opt} \approx 0.2$ per copper atom [1–3]. The compound with n_h^{opt} is said to be optimally doped. If the hole concentration n_h is less or more than the optimal one, we deal with an underdoped or overdoped compound, respectively. The thallium content and the oxygen depletion δ both define n_h in $Tl_2Ba_2Ca_nCu_{n+1}O_{6+2n-\delta}$.

As the inner CuO_2 plane is more distant from the acceptor TlO layer, a problem related to the hole distribution among crystallographically inequivalent planes arises. There are different view-points on this problem. Di Stasio et al. [4] have analysed the distribution of charge between the CuO_2 layers in the framework of a sheet charge model and pointed an important inhomogeneity of a hole distribution among crystallographically inequivalent CuO_2 planes for Tl2223. On the other hand taking into account a possible inhomogeneous distribution of charge within the layers Haines and Tallon [5] have calculated the equilibrium charge density distribution function and revealed that the degree of doping for the different CuO_2 planes is strongly dependent on the total concentration of holes in multilayered cuprates. According to these calculations a nearly homogeneous distribution of a charge among the planes is expected for Tl2223 with optimal n_h.

As established from NMR shift experiments, the temperature dependence of the uniform spin susceptibility of the CuO_2 layers $\chi_s(q=0, T)$ is very sensitive to the level of doping [6–8]. For the underdoped state ($n_h < n_h^{opt}$) the spin susceptibility χ_s decreases when lowering T. In the case of strongly overdoped compounds a monotonous increase of χ_s is observed. In the three layered oxide Bi2223, a substantially different behavior of $\chi_s(T)$ was found for inequivalent planes [9–11]. These data give evidence that the inner CuO_2 layer is less doped than the outer ones. A similar behavior of $\chi_s(T)$ was also found in $TlBa_2Ca_2Cu_3O_9$ compound [12]. The ^{17}O [13] and ^{63}Cu [14] NMR shift data, reported for TlBa2223 samples with $T_c = 114$ and 125 K, led the authors to conclude about a homogeneous hole distribution among the crystallographically inequivalent layers. It was suggested that as T_c^{opt} increases, the hole distribution among the different CuO_2 layers becomes more homogeneous in going from the underdoped Bi2223 and Tl1223 to Tl2223 with the highest T_c^{opt}.

The ^{63}Cu Knight shift at different copper sites changes with temperature in similar manner according to the data reported by Zheng et al. [15] for slightly overdoped Tl2223 ($T_c = 115$ K).

In our previous works [16,17] we reported the results of the combined analysis of the NMR line shift data on the ^{63}Cu, ^{17}O and ^{205}Tl nuclei in slightly overdoped Tl2223 with $T_c = 117\ K < T_c^{max}$ and optimal doped Tl2223 with $T_c = 123$ K. The temperature dependence of the uniform spin susceptibility $\chi_s(q=0)$ is found to be different for the crystallographically inequivalent CuO_2 layers. A rather sharp decrease of $\chi_s(T)$ with temperature occurs for the inner layer. This may be considered as an indication of the lower concentration of hole carriers in this layer in comparison with n_h for the outer layer. It is of interest to study by NMR the changes in the temperature dependence of $\chi_s(q=0)$ for crystallographically inequivalent CuO_2 layers in going from the overdoped towards the underdoped state of Tl2223. In the present paper we report the ^{63}Cu and ^{17}O NMR shift data obtained for uniaxially oriented ceramic samples of Tl2223 with $T_c = 117$ K (overdoped state) and $T_c = 104$ K (underdoped state) in normal and superconducting states.

2. Experimental technique and samples

The NMR measurements were performed on single-phase ceramic samples of $Tl_2Ba_2Ca_2Cu_3O_{10-\delta}$ with $T_c = 117$ K (sample 1) and with $T_c = 104$ K (sample 2). The first sample Tl2223 ($a = 3.8584$ Å, $c = 35.7058$ Å) was prepared by conventional solid-state reaction. The pure powders of BaO, $CaCO_3$ and CuO were mixed in the appropriate proportions with a pestle in an agate mortar. The product was heat treated at 850°C (30 h) and then at 920°C (40 h) with intermediate grindings. The obtained compounds were mixed with the appropriate amounts of Tl_2O_3

and pressed into pellets (13 mm in diameter). The pellets were wrapped in a nickel foil to prevent the loss of thallium at elevated temperatures and subsequent sintering was performed in a closed quartz tube in the following way: (a) two-stage heating up to 880°C for 45 min (in a dynamic vacuum up to 600°C at first and then in the oxygen atmosphere); (b) sintering at this temperature for 30 min; (c) cooling down to 750°C for 5 min and the final slow cooling to room temperature in the furnace.

X-ray diffraction data have shown that the materials prepared by the above procedure are almost single-phase. Thereby the admixture of the Tl2212 phase in the Tl2223 sample does not exceed 5%.

Then the ceramic pellets were powdered and enriched with ^{17}O isotope. The powder was poured into the platinum cup which was then placed into the quartz tube mounted in the furnace. Within this tube made in the form of the closed loop the $^{17}O_2$ was circulated. The starting enrichment accounted for 31.3%. During the heat treatment of the samples the oxygen gas in the loop was continuously scrubbed with Ascarite and cold plate (at 180 K). The ^{17}O–^{16}O isotope substitution was carried out at 650°C for 168 h under oxygen pressure of 730 Torr with three refillings of the system with 'fresh' oxygen-17. Then sample was cooled down at 15 K/h to room temperature. According to data of the mass spectroscopic analysis the final ^{17}O enrichment of the sample reaches 25%.

The value of T_c was determined as the temperature at which the diamagnetic response in the AC susceptibility measurements appears.

The synthesis and structural certification of sample 2 were reported in Ref. [18]. This sample was also enriched with oxygen-17 following to the procedure mentioned above. After enrichment sample 2 was first annealed in the nitrogen flow at 200°C for 3 h and then under vacuum (3 Torr) at 300°C for 5 h and, lastly, it was heat treated in a nitrogen atmosphere at 350°C for 5 h. The value of T_c has been decreased to $T_c = 104$ K after this procedure. X-ray analysis shows a single phase nature of the annealed sample. As a result of this heat treatment we found the lattice parameter a to be unchanged, viz $a =$ 3.8536 Å and a slight increase of the unit cell in the c-direction, namely $c = 35.689$ Å (before annealing) and $c = 35.767$ Å (after annealing). An increase of the lattice parameter c with decrease of T_c confirms the underdoped state of sample 2 [19].

Both powdered samples of Tl2223 were mixed with epoxy and oriented in the magnetic field of 8 T.

The ^{63}Cu and ^{17}O NMR measurements were carried out on Bruker NMR pulse spectrometer over the temperature range 10–400 K in a magnetic field $B_0 = 8$ T. The spectra were obtained with a $(\pi/2)_x$–τ-$(\pi/2)_y$–τ-(echo) pulse sequence and subsequent Fourier transform of the second half of the echo signal. The spin echo signals were measured after quadrature phase-sensitive detection with the discrete change of the spectrometer frequency. The total cycle of measurements was organized with successive 180°-alternation of rf phase for the first exciting pulse to eliminate distortions of spectra due to transient process in the rf circuit after pulse.

The components $K_{\perp(\parallel)}$ of the magnetic shift tensor for ^{63}Cu and ^{17}O were determined from the position of NMR line maximum corresponding to the central $(m = 1/2 \Leftrightarrow -1/2)$ transition by taking into account the second-order quadrupole corrections to the shift. We use the following notations for the ^{63}Cu magnetic shift components: $^{63}K_{\parallel}$ and $^{63}K_{\perp}$ are measured when B_0 is along the c-axis and in the ab plane, respectively. It should be noted that the value of $^{63}K_{\perp}$ depends strongly on the accuracy of determination of the quadrupole coupling constant of the copper nucleus. The related quadrupole frequencies $^{63}\nu_Q$ were obtained from the position of the maximums of the ^{63}Cu and ^{65}Cu NQR spectra measured at $T = 4.2$ K. At this temperature NQR line is broad and asymmetrical. Its width is more than 1 MHz which makes the precise determination of ν_Q difficult and thus of $^{63}K_{\perp}$. To reduce the error of $^{63}\nu_Q$ determination and to study its possible change with temperature, the spectrum of the central transition was also measured in a weaker magnetic field $B_0 =$ 3.9 T, since the frequency dependence of the quadrupole term $(\sim \nu_Q^2/\nu_0)$ and of the terms concerning the magnetic hyperfine interactions $(\sim \nu_0)$ contributing to the total shift of the ^{63}Cu NMR line are different. Analysing the spectra obtained at different ν_0 one could determine more accurately the values of $^{63}\nu_Q$ and $^{63}K_{\perp}$ for the whole range of temperatures. As a result we found that the change of ν_Q is less than 4% between 10–300 K. The quadrupole frequency $^{17}\nu_Q$ and an asymmetry param-

eter η for different oxygen sites were determined from the peak positions of the ^{17}O NMR lines related to $3/2 \Leftrightarrow 1/2$ and $-1/2 \Leftrightarrow -3/2$ satellite transitions.

As references we used a water solution of $CuSO_4$ for $^{63}Cu(^{63}\nu_L = 90.141$ MHz) and H_2O for $^{17}O(^{17}\nu_L = 46.101$ MHz).

3. Experimental results

3.1. ^{63}Cu NMR line shifts

For powder samples of $Tl_2Ba_2Ca_2Cu_3O_{10-\delta}$ the spectrum of the $1/2 \Leftrightarrow -1/2$ transition shows three peaks. An example of this spectrum measured early for Tl2223 ($T_c = 123$ K) can be seen on Fig. 1a. Two peripheral peaks are positioned in the same ranges of frequencies as for quadrupole splitted spectrum of Tl2212. A third additional peak appears at the centre of the spectrum. This peak is only slightly splitted at $B_0 = 8$ T. The total spectrum is interpreted as the superposition of two lines corresponding to the two sites Cu(1) and Cu(2) [16]. The line having the largest quadrupole splitting is attributed to the Cu(1)

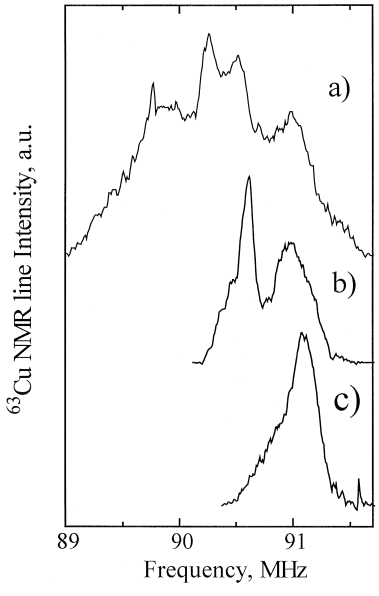

Fig. 1. The ^{63}Cu NMR spectra ($1/2 \Leftrightarrow -1/2$ transition) in the $Tl_2Ba_2Ca_2Cu_3O_{10-\delta}$ ($T_c = 123$ K) (a) unoriented powder, (b) oriented sample with $c \perp B_0$, (c) oriented sample with $c \| B_0$.

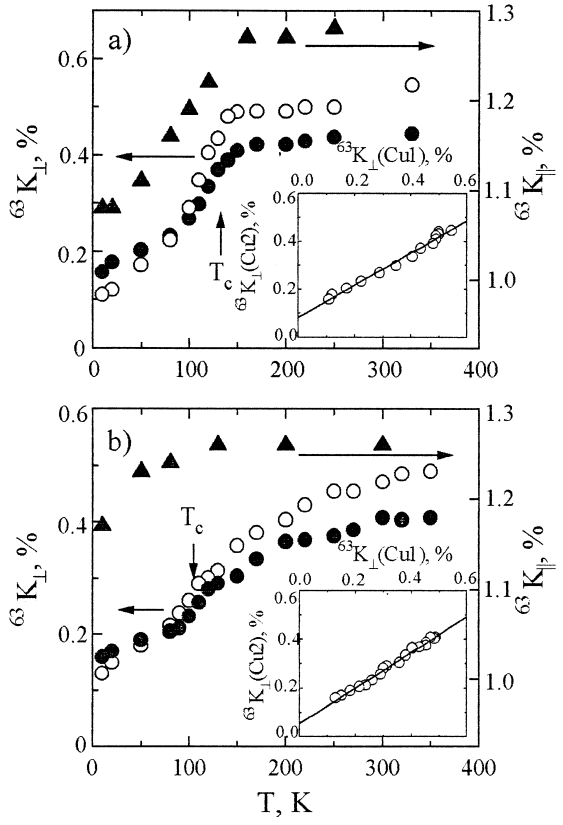

Fig. 2. The temperature dependencies of the ^{63}Cu NMR shift of Cu1 (open circle) and Cu2 (solid circle) position for $c \perp B_0$ and $c \| B_0$ in the $Tl_2Ba_2Ca_2Cu_3O_{10-\delta}$ with $T_c = 117$ K (a) and with $T_c = 104$ K (b). Plots $^{63}K_\perp$ (Cu2) vs. $^{63}K_\perp$ (Cu1) are shown at the insets for both samples.

atoms like for Tl2212. The second line with the smallest quadrupole splitting is due to the Cu(2) atoms. Its intensity is found to be about 40% of the intensity of the line with the larger quadrupole splitting. This ratio of intensities is quite reasonable, since the amount of Cu(2) in the inner CuO_2 layer is half of the amount of Cu(2) atoms in the outer CuO_2 layers.

Fig. 1b and c present the NMR spectra for the $m = 1/2 \Leftrightarrow -1/2$ transition in the oriented Tl2223 sample (with $T_c = 123$ K). In order to focus on the interesting peaks, we have omitted the part of the total ^{63}Cu spectrum lying below 90.3 MHz. An additional peak attributed to powder part of the sample is can be seen in this frequency domain. For $B_0 \perp c$ the spectrum has two peaks. The lines at the

lower frequency and at the higher frequency are assigned to Cu(2) and Cu(1) atoms, respectively.

The experimental error for $^{63}K_{\perp}$ at Cu(2) sites for both samples does not exceed 0.03%. The same error bar ($\pm 0.015\%$) can be put for the Cu(1) and Cu(2) data of sample 2. For sample 1 the important quadrupole broadening (≈ 150 kHz at $B_0 = 8$ T) and a poorer signal-to-noise ratio of the Cu(1) line increase the error for $^{63}K_{\perp}$(Cu1): $\Delta^{63}K_{\perp} \leq 0.04\%$ ($T < T_c$) and $\Delta^{63}K_{\perp} \leq 0.04\%$ ($T < T_c$).

The temperature dependencies of the magnetic shift $^{63}K_{\perp}$ for the Cu(1) and Cu(2) sites in the two samples of $Tl_2Ba_2Ca_2Cu_3O_{10-\delta}$ are presented in Fig. 2a,b.

For sample 1 ($T_c = 117$ K), at both copper sites the magnetic shift $^{63}K_{\perp}$ decreases slightly with temperature. A similar temperature dependence is observed in Bi2223 compound [11] for the Cu(1) and Cu(2) sites.

Our data concerning Cu(1) sites of sample 1 demonstrate a more flat T-dependence above $T = 130$ K than the reported recently by Zheng et al. [15] for Tl2223 with about the same T_c and measured with a higher precision at 10.6 T. But this difference is not an intrinsic property of our sample and is rather related to a problem of comparison of data measured with a different precision. As seen in the insets the plot of $^{63}K_{\perp}$(Cu2) vs. $^{63}K_{\perp}$(Cu1), can be fitted by a straight line within the experimental error. As we shall see below ^{17}K is a better probe than ^{63}K due to the better precision, for a more careful determination of the spin susceptibility.

In the case of sample 2 with the larger oxygen depletion, a stronger temperature dependence of the Cu NMR line shift takes place in the normal state.

The shift $^{63}K_{\perp}$ for both lines also drops below T_c. This drop is more pronounced in overdoped sample, it is due to the freezing of the spin contribution $^{63}K_s$ which is proportional to uniform part of the spin susceptibility $\chi_s(q = 0)$. For copper in the CuO_2 layers the shift $^{63}K_s = H_{hf}\chi_s(q=0)$ demonstrates a rather strong anisotropy ($^{63}K_{s\perp} > {}^{63}K_{s\parallel}$) due to the anisotropy of the magnetic hyperfine fields H_{hf} at the Cu nuclei. In the superconducting state one has to take into account the diamagnetic contribution K_{dia} to total NMR shift. As estimated for $B_0 = 8$ T and $T = 10$ K $\ll T_c$ this diamagnetic correction $|K_{\perp dia}|$ is about 0.005%, that is markedly less than an error ΔK in determination of $^{63}K_{\perp}$. Evaluating the spin contribution we assumed $K_{s\perp} = 0$ at $T = 10$ K $\ll T_c$. In this case the difference $K_{\perp}(T) - K_{\perp}(T = 10\ \text{K})$ can be accounted as a measure of $K_{s\perp}(T)$. The values of $K_{s\perp}(T \cong T_c)$ for both Cu1 and Cu2 positions of the samples under study are listed in Table 1.

For $B_0 \| c$ the lines of different copper sites are resolved very poorly and form a single asymmetric line.

Table 1
The structural parameters, as well as the quadrupole frequencies and the asymmetry parameters for the $Tl_2Ba_2Ca_2Cu_3O_{10-\delta}$ ($T_c = 117$ K, $T_c = 123$ K, $T_c = 104$ K)

	$T_c = 117$ K		$T_c = 123$ K[a]		$T_c = 104$ K	
a (Å)	3.858(9)		3.851(2)		3.853(4)	
c (Å)	35.705(6)		35.720(1)		35.767(8)	
	$Cu(1)O_2$	$Cu(2)O_2$	$Cu(1)O_2$	$Cu(2)O_2$	$Cu(1)O_2$	$Cu(2)O_2$
$^{63}\nu_Q$ (MHz)	17.2(3)	11.4(3)	16.5(3)	10.8(3)	14.3(2)	10.0(2)
$^{63}K_{orb\perp}$ (%)	0.11(3)	0.16(3)	0.15(3)	0.20(3)	0.13(2)	0.16(2)
$^{63}K_{s\perp}(T \cong T_c)$ (%)	0.29(5)	0.16(4)	0.25(5)	0.14(3)	0.16(3)	0.10(2)
$^{63}K_{s\parallel}(T \cong T_c)$ (%)	0.18(3)	< 0.18	–	–	0.09(3)	< 0.09
$^{17}\nu_Q$ (MHz)	1.10(5)	1.10(5)	–	–	0.94(5)	0.94(5)
$^{17}\eta$	0.33(1)	0.33(1)	–	–	0.30(1)	0.30(1)
$^{17}\sigma\perp$ (%)	0.20(5)	0.020(5)	–	–	0.020(5)	0.020(5)
$^{17}K_{s\perp}$ (%)	0.10(2)	0.09(2)	–	–	0.09(2)	0.09(2)

[a] For optimal doped sample of Tl2223 with $T_c = 123$ K the $^{63}\nu_Q$ frequencies were measured at both crystallographically inequivalent sites of copper in our previous work [16].

At $T = 250$ K the shifts $^{63}K_{\parallel}$ is equal to 1.29(5) and 1.26(5)% for sample 1 and 2, respectively. As seen in Fig. 2, $^{63}K_{\parallel}$ decreases slightly when lowering T and its value at $T = 10$ K is 1.09(5) and 1.15(5)% for sample 1 and 2, respectively. A similar thermal behavior of $^{63}K_{\parallel}$ is reported in Ref. [15] for Tl2223 with $T_c = 115$ K.

For $^{63}K_{\parallel}$, the diamagnetic correction increases and reaches $|K_{\parallel dia}(T \ll T_c)| \approx 0.025\%$ for $B_0 = 8$ T. As seen in Fig. 2 the variation of $^{63}K_{\parallel}$ in superconducting state exceeds this value which is approximately equal to the error of the shift measurements in our experiments.

3.2. ^{17}O NMR line shifts

The whole ^{17}O NMR spectra of the magnetically oriented powder of Tl2223 are shown in Fig. 3a,b. The spectra were obtained at $T = 120$ K for c parallel (a) and perpendicular (b) to the magnetic field B_0. The shape of spectra is very similar to those reported for oriented powders of thallium compounds with one (TlBa2201) [20], two (TlBa2212) [21] and three (TlBa2223, $T_c = 115$ K) [15] CuO_2 planes. We use the same notations as in Refs. [20,21] for peaks of the satellites lines of oxygen placed at different sites.

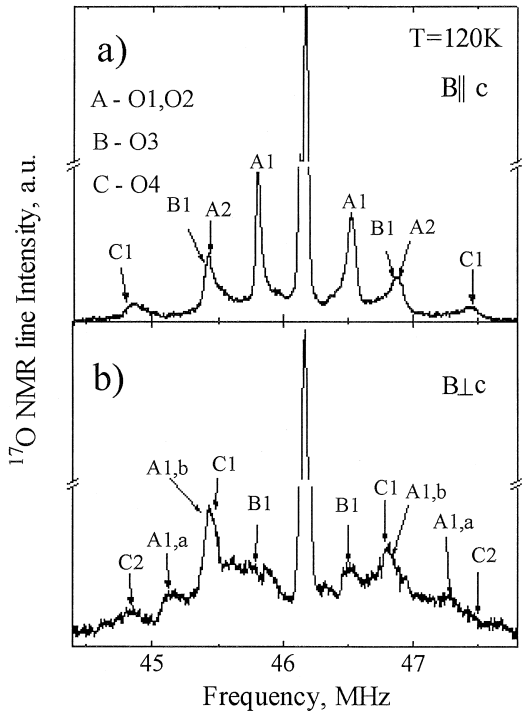

Fig. 3. The ^{17}O NMR spectra of the oriented Tl2223 ($T_c = 117$ K) for $c \| B_0$ (a) and $c \perp B_0$ (b).

The assignment of the different lines in the ^{17}O NMR spectra was done in our previous paper [21]. Here the discussion will be restricted to the 'A'-lines, having a strong temperature dependence of their positive shift and corresponding to oxygen O1 and O2 in the outer and inner CuO_2 layers, respectively. For these oxygen atoms the principal axis of the electric field gradient (EFG) tensor lies in the a–b plane along the Cu–O–Cu bond.

The quadrupolar frequencies $^{17}\nu_Q$ and asymmetry parameters η for these different oxygen positions were calculated from the peak positions of the NMR lines corresponding to the $\pm 3/2 \Leftrightarrow \pm 1/2$ transitions with different orientation of the c-axis with respect to B_0.

For example, for the $m = +3/2 \Leftrightarrow +1/2$ transition the A1 peak should be in agreement with the frequency ν_1 defined by the expression [22] for the orientation of c along the B_0:

$$\nu_1 = \nu_0(1 + K_\perp) \pm \frac{1}{2}\nu_Q(1 - \eta) + \frac{5\nu_Q^2}{16\nu_0}\left(1 + \frac{2}{3}\eta + \frac{1}{9}\eta^2\right). \quad (1)$$

For B_0 aligned in the a–b plane a 'double peak' line should appear for uniaxially oriented powder with two singularities at ν_2 and ν_3:

$$\nu_2 = \nu_0(1 + K_\perp) \pm \frac{1}{2}\nu_Q(1 + \eta) + \frac{5\nu_Q^2}{16\nu_0}\left(1 - \frac{2}{3}\eta + \frac{1}{9}\eta^2\right), \quad (2)$$

$$\nu_3 = \nu_0(1 + K_\parallel) \mp \nu_Q + \frac{5\nu_Q^2}{36\nu_0}\eta^2. \quad (3)$$

We assume in Eqs. (1)–(3) an axial symmetry of the magnetic shift tensors for the ^{17}O NMR lines, denoting the components $K_a \equiv K_\parallel$, $K_b = K_c \equiv K_\perp$ for the Cu–O–Cu fragment which is located along the a-axis.

This assumption is very close to real structure of magnetic shift tensor at O1 and O2 sites. As shown in the ^{17}O NMR experiments in single crystals of Y123 [23] and in oriented powder of Tl2223 [15] the difference $|^{17}K_b - {}^{17}K_c| \ll {}^{17}K_c$ for oxygen in CuO_2 layer.

No sizeable additional peaks in the pattern of satellites were found in going from Tl2212 to Tl2223. This means that within the error of determination for $^{17}\nu_Q$($\Delta^{17}\nu_Q = \pm 40$ kHz) the EFG has about the same value at oxygen placed in the structurally inequivalent copper layers.

The values of ν_Q and η obtained for oxygen in both samples are listed in Table 1.

For sample 1 the value of $^{17}\eta$ is a little less than the one reported in Ref. [15] and $^{17}\nu_Q = 1.10(5)$ MHz is can be considered as the average weighted of $^{17}\nu_Q$(O in inner CuO_2 layer) = 1.06 MHz and $^{17}\nu_Q$(O in outer CuO_2 layer) = 1.12 MHz [15] obtained for Tl2223 with $T_c = 117$ K.

The O1 and O2 central line ($-1/2 \Leftrightarrow 1/2$ transition) changes markedly its shape in going from the overdoped sample 1 to the underdoped sample. In sample 1 this line demonstrates a shape with 'two humps' for $c \| B_0$ orientation (Fig. 4a), as distinct from the apparent single gaussian line in sample 2 (Fig. 4b). We believe that the splitting of the line in sample 1 evidences the difference in the magnetic shifts for oxygen in the inner and the outer CuO_2 layers.

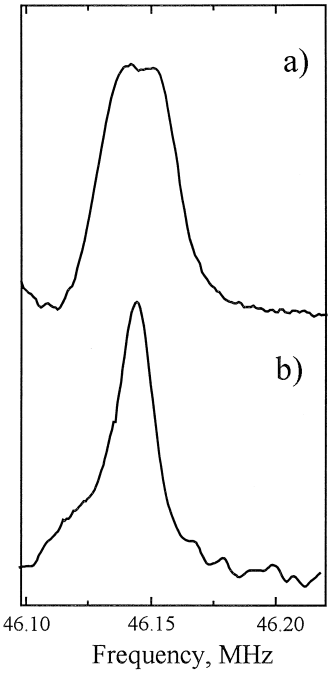

Fig. 4. The ^{17}O NMR spectra of the $1/2 \Leftrightarrow -1/2$ central transition for $c \| B_0$ in Tl2223 with $T_c = 117$ K (a) and $T_c = 104$ K (b).

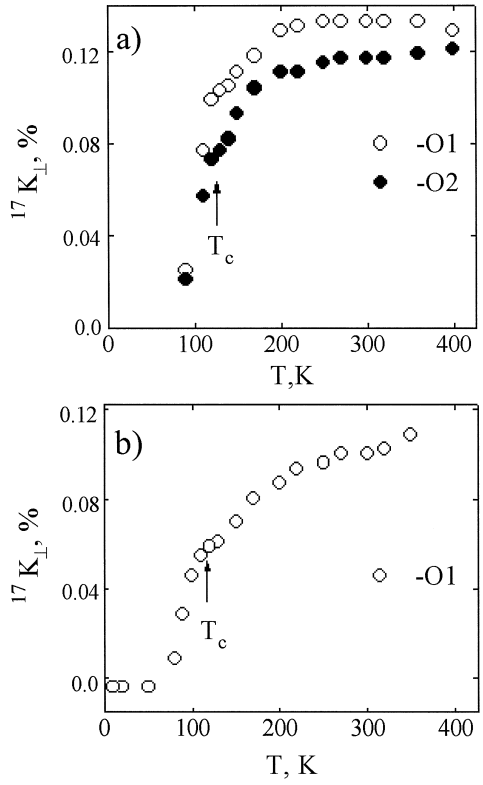

Fig. 5. The temperature dependence of the ^{17}O NMR shift of O1 (open circle) and O2 (solid circle) in Tl2223 with $T_c = 117$ K (a) and $T_c = 104$ K (b) for $c \| B_0$.

For sample 2, the difference between the shifts of the O1 and O2 lines vanishes. Thereby a narrower single central NMR line of ^{17}O is observed in the normal and superconducting states. The central line was simulated with two Gaussians having different shift of maxima and the results for $K_\perp$ at O1 and O2 positions for both samples are presented in Fig. 5a,b. For sample 1, the magnitude of $^{17}K_\perp$(01) is the

largest and its value reaches a maximum at room temperature. For O2 in the middle copper layer a gradual monotonous decrease of $^{17}K_{\perp}(02)$ with temperature is observed without any maximum. For sample 2 the slope of $^{17}K_{\perp}(T)$ is steeper than in sample 1 as usually found in less doped cuprates. It is worth to note that although sample 1 is overdoped $^{17}K_{\perp}$ decreases when lowering T as it is often found for not too strongly overdoped compounds [20].

4. Discussion

Magnetic hyperfine interactions contributing to the ^{63}Cu and ^{17}O NMR shifts were well studied in cuprates and reviews on this topic can be found in Refs. [24–27]. In the normal state the total magnetic shift can be written as:

$$K(T) = \sigma + K_{\mathrm{orb}} + K_{\mathrm{s}}(T), \quad (4)$$

$$K_{\mathrm{s}}(T) = H_{\mathrm{hf}}\chi_{\mathrm{s}}(T). \quad (5)$$

The first term in Eq. (4) is the chemical shift σ which is due to magnetic hyperfine interaction of the ^{17}O nuclei with electrons of closed shells. For Cu atoms the orbital contribution K_{orb} of the partially filled 3d-orbitals appears. This contribution is due to the Van Vleck paramagnetism of the 3d shells of copper and exceeds substantially the chemical shift. K_{orb} and σ may be considered as independent of the temperature. Thus the temperature dependence of the

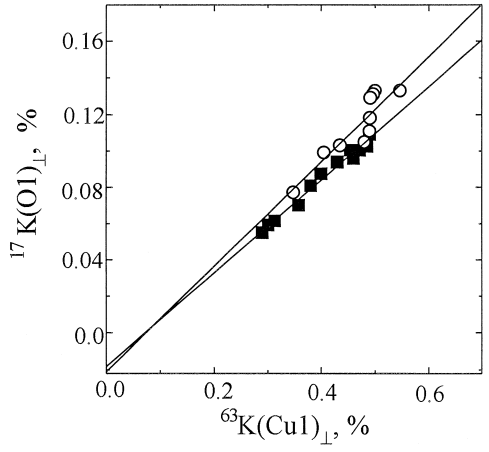

Fig. 6. $^{17}K_{\perp}$ (O1) vs. $^{63}K_{\perp}$ (Cu1) with temperature as a parameter for the normal state of $Tl_2Ba_2Ca_2Cu_3O_{10-\delta}$ ($T_c = 117$ K) (○) and $Tl_2Ba_2Ca_2Cu_3O_{10-\delta}$ ($T_c = 104$ K) (■).

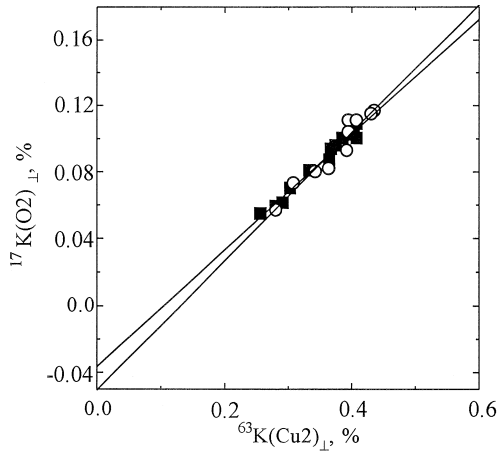

Fig. 7. $^{17}K_{\perp}$ (O2) vs. $^{63}K_{\perp}$ (Cu2) with temperature as a parameter for the normal state of $Tl_2Ba_2Ca_2Cu_3O_{10-\delta}$ ($T_c = 117$ K) (○) and $Tl_2Ba_2Ca_2Cu_3O_{10-\delta}$ ($T_c = 104$ K) (■).

total shifts is due to the spin contribution K_{s}, which is caused by the magnetic hyperfine interaction with electrons of the conduction band (Knight shift). This shift is proportional to the local spin susceptibility $\chi_{\mathrm{s}}(T)$ through the hyperfine field H_{hf}.

The NMR data on the nuclei in the copper layer are well described for a considerable number of cuprates $YBa_2Cu_3O_7$, $La_{2-x}Sr_xCuO_4$ [28–31] in terms of the single spin susceptibility in the layer. By this assumption the Knight shifts of oxygen and copper positioned in the same layer are expected to change with temperature proportionally to each other in accordance with Eq. (4). Figs. 6 and 7 show the plots of $^{17}K_{\perp}(01)$ vs. $^{63}K_{\perp}$ (Cu1) and $^{17}K_{\perp}(02)$ vs. $^{63}K_{\perp}$ (Cu2) with temperature as a parameter for sample 1 and 2. Such a proportionality allows one to use the single spin liquid picture, developed in Refs. [28–31].

In order to check the applicability of the single spin susceptibility approximation to multilayered cuprates it is necessary to compare the temperature dependencies of magnetic shift for atoms positioned in the different CuO_2 layers. The ^{17}O NMR shift data measured with a better precision ($\Delta^{17}K \leq 0.004\%$) are more suitable for this task. For sample 2 the same value of ^{17}K was found at O1 and O2 sites for all temperatures under study and this permits to describe at small wave vectors $\boldsymbol{q}$ the electron states in the different CuO_2 planes with a unique spin

susceptibility. The situation changes when increasing the doping. In sample 1, the plot of $^{17}K(O1)$ vs. $^{17}K(O2)$ (○) (Fig. 8) cannot be described by a straight line starting from the origin of coordinates $^{17}K(O1) = {}^{17}K(O2) = 0$. As will be discussed below, the chemical shifts for oxygen from different copper layers are equal to one another $^{17}\sigma_{\perp}(O1) \approx {}^{17}\sigma_{\perp}(O2)$ and the very same fit would be expected if both types of CuO_2 layers were described with the same χ_s.

Now we refer to the ^{17}O and ^{63}Cu NMR shift data obtained for sample 2 with $T_c = 104$ K. The NMR line of the central transition for oxygen (Fig. 4b) demonstrates a nonsplitted symmetrical shape as distinct from the overdoped Tl2223.

This shape remains unchanged when T decrease. It was not possible to separate the contributions of the O1 and O2 sites to this line. In sample 2, the identical thermal behavior of the oxygen lines with temperature makes possible in accordance with Eqs. (4) and (5) to assume $^{17}\sigma_{\perp}(O1) \approx {}^{17}\sigma_{\perp}(O2)$ and $^{17}K_s(O1) = {}^{17}K_s(O2)$ for oxygen placed in the crystallographically inequivalent CuO_2 layers. It is reasonable to suppose that hyperfine fields at the oxygen atoms in different layers are the same: $^{17}H_{hf\perp}(O1) = {}^{17}H_{hf\perp}(O2)$, since its magnitude is monitored by Cu–O–Cu distance in plane. Thus the ^{17}O NMR data demonstrate the decrease of $\chi_s(q = 0)$ and its unified temperature dependencies for inequivalent CuO_2 planes in Tl2223 when reducing the concentration of holes $n_h < n_h^{opt}$.

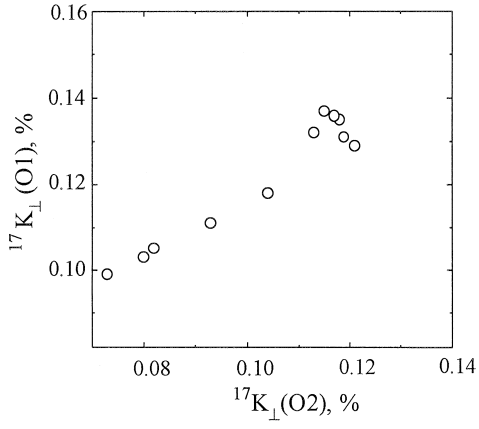

Fig. 8. $^{17}K_{\perp}(O1)$ vs. $^{17}K_{\perp}(O2)$ with temperature as a parameter for the normal state of $Tl_2Ba_2Ca_2Cu_3O_{10-\delta}$ ($T_c = 117$ K).

The central lines corresponding to Cu1 and Cu2 being well resolved for $B_0 \perp c$. One can trace separately NMR shift of copper in the inner and the outer CuO_2 layers. For sample 2 the plot of $^{63}K(Cu2)$ vs. $^{63}K(Cu1)$ with a temperature as a parameter is fitted satisfactorily by a straight line (inset Fig. 2b) indicating that a single spin susceptibility may be applied to describe electronic states at $\boldsymbol{q} = (0; 0)$ in different CuO_2 planes of underdoped Tl2223. In these planes the Cu1 and Cu2 atoms have a different nearest oxygen surrounding and the distinction in magnitude of $^{63}K_{\perp}$ and in its slope with temperature for Cu1 and Cu2 can be attributed to different values of $^{63}K_{orb\perp}$ and $^{63}H_{hf\perp}$ in structurally inequivalent planes.

According to Zheng et al. [15] the difference in magnitude of $^{63}K_{\perp}$ between pyramidal and square planes is attributed to the difference in spin susceptibility at $q = 0$. In this case the ratio of $K_s(Cu1)/K_s(Cu2)$ is expected to approach at elevated temperatures the 3D paramagnet limit $K_s(Cu1)/K_s(Cu2) = 1$. Here the equality as $^{63}H_{hf\perp}(Cu1) = {}^{63}H_{hf\perp}(Cu2)$ is assumed. Only ^{17}K demonstrate this tendency as seen in Fig. 5. The $^{63}K_{\perp}$ presented in this work and reported in Ref. [15] do not reveal such a tendency indicating that a difference in magnitudes of $^{63}H_{hf\perp}(Cu1)$ and $^{63}H_{hf\perp}(Cu2)$ might be involved in discussion of the $^{63}K_{\perp}$ ratio.

Thus according to the ^{63}Cu and ^{17}O NMR data $\chi_s(q = 0, \omega = 0)$ decreases with T and its temperature dependence becomes the same for the inequivalent CuO_2 layers in going towards an underdoped state of multilayered cuprate Tl2223. As we have mentioned the decrease of n_h enhances the pseudogap-like drop of χ_s above T_c and we may enlarge our conclusion as follows. In going to the underdoped state of Tl2223 a more homogeneous distribution of hole carriers occurs among the crystallographically different layers of CuO_2.

Further, we turn back to the expressions (4) and (5) and give some estimations for different contributions to the total NMR shift. We have already found $^{17}\sigma_{\perp} = 0.020(5)\%$ [21] for oxygen placed in the CuO_2 layer of $Tl_2Ba_2CaCu_2O_{8-\delta}$ by analysing jointly the ^{17}O and ^{205}Tl NMR shift data. The same values of $\sigma_{\perp}$ can be taken for oxygen in the outer copper layers of Tl2223 since the Cu1–O1 distance and symmetry of the nearest environment of the Cu

atoms are the same as in Tl2212. Using the plot of ^{17}K(O1) vs. ^{63}K(Cu1) (Fig. 6) the value of the orbital shift $^{63}K_{\mathrm{orb}\perp} = 0.11\%$ is obtained for Cu1 in sample 1. The same procedure applied to the O1–Cu1 data for sample 2 with $T_c = 104$ K yields $^{63}K_{\mathrm{orb}\perp} = 0.13\%$. The orbital shift for Cu2 was found to be slightly increased for both samples ($^{63}K_{\mathrm{orb}\perp}$(Cu2) = 0.16%) in comparison with values obtained for Cu1 sites.

Considering the ^{63}Cu NMR shifts data far below T_c (Fig. 2a,b) one can note that the experimental value of the line shift $^{63}K_{\perp}$(10 K) is very close to $^{63}K_{\mathrm{orb}}$ obtained as a result of the fitting. Thus we conclude that the additional diamagnetic contribution to the ^{63}Cu and ^{17}O NMR line shifts below T_c, does not exceed 0.005% when $B_0 \perp c$ and $B_0 = 8$ T. For $B_0 \| c$ the value of $K_{\mathrm{dia}\|} = -0.025\%$ was obtained as a difference between experimental value of the ^{17}O NMR line shift at $T = 10$ K and the chemical shift $^{17}\sigma_{\perp} = 0.02\%$.

The experimental values of the quadrupole frequencies ν_Q and the asymmetry parameters η for ^{63}Cu and ^{17}O nuclei (see Table 1) obtained in the present paper allow us to estimate the hole occupation numbers at Cu and oxygen sites in the CuO_2 planes of Tl2223.

It should be noted that in both Cu sites, Cu1 and Cu2, the values of quadrupole frequency

$$^{63}\nu_Q = \frac{3e^{63}Q}{2I(2I-1)h} q_{zz} \tag{6}$$

increase when the hole doping level increase. This increase is related to change of the so-called valence contribution to the total electric field gradient q_{zz}. According to Schwarz et al. [32], Ambrosch et al. [33] and Yu et al. [34] the value of the lattice contribution q_{zz}^{lat} at the Cu sites accounts for only 1–5% of the total q_{zz}. Then the following relation may be written:

$$q_{zz} = q_{zz}^{\mathrm{val}} + q_{zz}^{\mathrm{lat}} \approx q_{zz}^{\mathrm{val}}. \tag{7}$$

The valence contribution at the Cu sites is defined by the contributions from the electrons in the Cu 4p-orbit and holes in the Cu $3d_{x^2-y^2}$ orbit:

$$q_{zz}^{\mathrm{vol}} = q_{zz4p} + q_{zz3d} = e(4/5)\langle r^{-3}\rangle_{4p} \times \left(n_{4p,z} - \frac{n_{4p,x} + n_{4p,y}}{2} \right) \times + e(4/7)\langle r^{-3}\rangle_{3d} n_{x^2-y^2}, \tag{8}$$

where $n_{4p,\alpha}$ and $n_{x^2-y^2}$ are the electron number in the Cu 4p-orbit and hole number in the Cu $3d_{x^2-y^2}$ orbit, respectively. The presence of two terms in Eq. (8) makes difficult at first sight the analysis of the variations with doping of partial contributions of 4p- and 3d-states to ν_Q (Eq. (6)) in doping. To estimate $n_{4p,\alpha}$ Hanzawa [27] proposed the following empirical relation:

$$n_{4p,\alpha} = \frac{C}{R_{\mathrm{Cu-O},\alpha} - R_0} - 0.0377, \tag{9}$$

where $C = 0.0297$ Å, $R_0 = 1.626$ Å. The distance $R_{\mathrm{Cu-O},\alpha}$ between Cu and the nearest oxygen was determined using X-ray diffraction data (see Table 1). The Cu–O-distance in plane does not change under doping within experimental accuracy. Since $n_{4p,z} \ll (n_{4p,x}, n_{4p,y})$ its possible variation due to small change of $R_{\mathrm{Cu-O4}}$ distance is expected to be negligible. Therefore, we assume that total EFG at copper changes due to variations of $n_{x^2-y^2}$ only (second term in Eq. (8)). Using the value $\langle r^{-3}\rangle_{4p} = 25.73$ a.u. [34] and the known values for $R_{\mathrm{Cu-O},\alpha}$ in Tl2223 we can find from the expressions (6–9) the concentrations of 4p-electrons $n_{4p,\alpha}$ and the contributions to the quadrupole frequency $\nu_{4p,z}$ from 4p-electrons for the Cu1 and Cu2 sites (Table 2).

Table 2
Values of $R_{\mathrm{Cu-O},\alpha}$, concentration of 4p-electrons in $4_{p,\alpha}$-orbits and 4p-electron contribution to the quadrupole frequencies of different Cu sites for Tl2223

	$\nu_{4p,z}$ (MHz)	$R_{\mathrm{Cu-O1}}$ (Å)	$R_{\mathrm{Cu-O2}}$ (Å)	$R_{\mathrm{Cu-O4}}$ (Å)	$n_{4p,x}$	$n_{4p,y}$	$n_{4p,z}$
Cu1	−28.27(9)	1.925	1.925	2.302	0.0616(5)	0.0616(5)	0.0061(7)
Cu2	−31.62(9)	1.924	1.924	–	0.0620(5)	0.0620(5)	0

Then using $\langle r^{-3}\rangle_{3d} = 8.2687$ a.u., the Hartree–Fock value for $3d^9$ configuration [35], experimental values of quadrupole frequencies of copper ν_Q and values obtained $\nu_{4p,z}$, from the expressions (6–8) we find the hole numbers $n_{x^2-y^2}$ of the Cu 3d-orbits for the Cu1 and Cu2 sites in Tl2223 with different doping degree (see Table 3).

The holes in $2p_\sigma$- and $2p_\pi$-orbits of oxygen are the main contribution to electric field gradient for oxygen positions. The hole numbers in these orbits $n_{p\sigma}$ and $n_{p\pi}$ may be found from the following expressions [36]:

$$n_{p\sigma} = \left(1 + \frac{\eta}{3}\right)\frac{\nu_z}{\nu_{2p,0}}, \tag{10}$$

$$n_{p\pi} = \frac{2}{3}\eta\frac{\nu_z}{\nu_{2p,0}}, \tag{11}$$

where $\nu_{2p,0} = (3/20)(e^2Q/h)(4/5)\langle r^{-3}\rangle_{2p}$ is the contribution from one hole in the p-orbit. The values of $n_{p\sigma}$ and $n_{p\pi}$ for overdoped and underdoped states of Tl2223 are presented in Table 3.

One of important quantities is the concentration of holes δn doped into molecular orbit O2p–$Cu3d_{x^2-y^2}$–O2p of the CuO_2 layer. In accord with Ref. [27] the quantity δn can be written in the following form:

$$\delta n = n_{x^2-y^2} - n_{4s} - \sum_\alpha n_{4p,\alpha} + 2(n_{2p\sigma} + n_{2p\pi}) + 2n_{2s} - 1, \tag{12}$$

where n_{4s} and n_{2s} are the electron numbers in the 4s-orbit of copper and hole numbers in 2s-orbit of oxygen, respectively; unity in Eq. (12) corresponds to the half-filled state with respect to the $2d^{10}$ state. The values $n_{4s} = 0.07$ and $n_{2s} = 0.141$ have been taken from the paper [27] for $YBa_2Cu_3O_7$. The obtained values of δn are presented in Table 3.

It should be noted that the value obtained for the contribution $\nu_{4p,z}$ in Refs. [32–34] is considerably different from the value $\nu_{4p,z} = -69$ MHz obtained in Ref. [37] on the basis of a cluster model for $YBa_2Cu_3O_6$. If the data presented in Ref. [37] are used in line with the calculation scheme above other values of $n_{x^2-y^2}$ and δn can be obtained (see Table 3). In this case our results for $n_{x^2-y^2}$, $n_{p\sigma}$ and $n_{p\pi}$ in the outer CuO_2 layer of the overdoped Tl2223 are in fairly good agreement with the values obtained in Ref. [36] for Tl2223 with $T_c = 115$ K (see Table 1 in Ref. [36]). The difference in the values of δn can be due to the fact that we have additionally taken into account the electron numbers in the Cu 4s-orbits and hole numbers in the O 2s-orbits. Unfortunately, it is hard to say which values of $n_{x^2-y^2}$ and δn approximate to the truth. However, independent of the value of the contribution $\nu_{4p,z}$ to the quadrupole frequency of the Cu nuclei ν_Q one can trace the tendency of the change of the hole numbers $n_{x^2-y^2}$ in the Cu 3d-orbit and concentration of doped holes δn in molecular O2p–$Cu3d_{x^2-y^2}$–O2p-orbit for each of inequivalent CuO_2 layers depending on the doping degree of Tl2223. The data presented in Table 3 show that: (i) in the underdoped state of Tl2223 ($T_c = 104$ K) the hole numbers $n_{x^2-y^2}$ and concentration of doped holes δn in the inner and outer CuO_2 layers are close to each other; (ii) with the growth of doping degree the quantities $n_{x^2-y^2}$ and δn are increased in each of the CuO_2 layers; (iii) with the growth of the total number of holes the difference in the number of doped holes δn between inequivalent CuO_2 layers is increased: the hole number in outer layer δn(Cu1) is increased with doping

Table 3
Hole numbers in the copper $3d_{x^2-y^2}$- and oxygen 2p-orbits and concentrations of doped holes δn in structurally inequivalent CuO_2 layers. The values of n_i are given on per atom basis

	$\nu_{4p,z}$ (MHz)	Tl2223 ($T_c = 117$ K)				Tl2223 $T_c = 123$ K	Tl2223 ($T_c = 104$ K)			
		$n_{x^2-y^2}$	$n_{p\sigma}$	$n_{p\pi}$	δn	$n_{x^2-y^2}$	$n_{x^2-y^2}$	$n_{p\sigma}$	$n_{p\pi}$	δn
$Cu(1)O_2$	−28.3	0.388	0.335	0.066	0.272	0.382	0.363	0.284	0.051	0.117
$Cu(2)O_2$	−31.6	0.367	0.335	0.066	0.251	0.363	0.355	0.284	0.051	0.114
$Cu(1)O_2$	−69	0.735	0.335	0.066	0.456	0.730	0.710	0.284	0.051	0.298
$Cu(2)O_2$	−72.1	0.712	0.335	0.066	0.440	0.707	0.700	0.284	0.051	0.297

faster than that in inner layer δn(Cu2); (iv) the values of the ratio $n_{x^2-y^2}/(n_{p\sigma}+n_{p\pi})$ in Tl2223 decreases in increasing the doping degree. This gives evidence that the holes doped into the CuO_2 layers are mainly located in the orbits of the oxygen atoms.

Now we attempt to estimate the real concentration of mobile hole carriers n_h in both types of CuO_2 layers avoiding the difficulty of conclusive determination of the contribution $\nu_{4p,z}$. As noted previously we assume that the concentration of the 4p-electrons, n_{4p}, is independent of the doping degree and that $n_{x^2-y^2}$ are proportional to the concentration of mobile holes n_h in CuO_2 layer.

Thus we suppose that the structure of the hole carriers wave function does not change in considerable extent under doping around maximum of T_c. As a result $^{63}\nu_Q$ should increase linearly with n_h in the CuO_2 plane [27,38] and the slope of this increase is the same for both planes. This slope is independent of the doping degree of the compound

$$\frac{d\nu_Q(Cu1)}{dn_h(Cu(1)O_2)} = \frac{d\nu_Q(Cu2)}{dn_h(Cu(2)O_2)}. \tag{13}$$

In order to find this slope we need a value of $\langle n_h \rangle$ (which is the average hole carriers concentration measured in galvanic–magnetic experiments) for both samples. Unfortunately we have no macroscopic measurements related to $\langle n_h \rangle$. The Hall carrier densities $1/(eR_H) = p_H$ were reported in Refs. [39,40] for optimally doped sample of Tl2223 with $T_c = 122$ K ($< n_h^{opt} > = 0.15$ hole/Cu atom) and for the underdoped one with $T_c = 102$ K (this value is very close to the one obtained for sample 2). We followed nearly the same preparation procedure in sintering the underdoped sample 2 as used in Refs. [39,40] for Tl2223 ($T_c = 102$ K). Therefore, we assume the average hole concentration for sample 2 equal to $\langle n_h^{un} \rangle \cong 0.09$ hole/Cu as should be obtained for Tl2223 with $T_c = 102$ K [39,40]. As shown above for sample 2 the holes are uniformly distributed among the inequivalent CuO_2 layers, viz $n_h^{un}(Cu(1)O_2) = n_h^{un}(Cu(2)O_2) = 0.09$ hole/Cu atom. For optimally doped sample we set the average hole concentration equal to and $\langle n_h^{opt} \rangle \cong 0.15$ hole/Cu atom as is obtained for Tl2223 with $T_c = 122$ K [39,40]. And the following expressions can be written to estimate $d^{63}\nu_Q/dn_h(CuO_2)$:

$$\langle n_h^{opt} \rangle = \tfrac{1}{3}\left(2n_h^{opt}(Cu(1)O_2) + n_h^{opt}(Cu(2)O_2)\right), \tag{14}$$

$$\frac{\nu_Q^{opt}(Cu1) - \nu_Q^{un}(Cu1)}{n_h^{opt}(Cu(1)O_2) - n_h^{un}(Cu(1)O_2)} = \frac{\nu_Q^{opt}(Cu2) - \nu_Q^{un}(Cu2)}{n_h^{opt}(Cu(2)O_2) - n_h^{un}(Cu(2)O_2)}. \tag{15}$$

The slope of $^{63}\nu_Q$ vs. $n_h(CuO_2)$ for Tl2223 is found to be equal 29 MHz/hole for both Cu1 and Cu2. The value of the slope $d^{63}\nu_Q/dn_h(CuO_2)$ obtained for the five-fold coordinated copper in the case of $YBaCuO_{6+x}$ is equal to 23.4 MHz/hole [38]. The difference is not so large and for detailed discussion one needs to measure NMR and transport properties at the same samples. As a result the concentration of holes in inequivalent layers is found to be different for optimally doped Tl2223: $n_h^{opt}(Cu(1)O_2) = 0.166$ hole/Cu atom, $n_h^{opt}(Cu(2)O_2) = 0.118$ hole/Cu atom, $d\nu_Q/dn_h = 29$ MHz/hole. For the overdoped sample 1 this difference is increased. We obtain $n_h^{ov}(Cu(1)O_2) = 0.190$ hole/Cu atom and $n_h^{ov}(Cu(2)O_2) = 0.138$ hole/Cu atom.

For multilayered cuprates having inequivalent copper layers it was pointed by Haines and Tallon [5], that a coulomb interaction of holes with ionic core leads to the inequality $n_h(Cu(1)O_2) > n_h(Cu(2)O_2)$ for the overdoped state. This inequality is weakened with reduction of the hole concentration and may go into the opposite one, namely $n_h(Cu(1)O_2) < n_h(Cu(2)O_2)$, in the case of strongly underdoped state. Our results support these calculations in general. However, according to our estimation the carrier concentration $n_h(Cu(2)O_2)$ in the inner CuO_2 layer is reduced when decreasing the total number of holes in the sample, which is contrary to the increase of this value predicted in Ref. [5] (Fig. 9, solid line). This discrepancy may be explained in the following way. As known the real content of Tl in the thallium layers is less than two atoms of Tl per formula unit. Haines and Tallon did not consider this depletion of the thallium sublattice. They also did not take into account that some amount of thallium ($\sim$ 5–9%) substitute for calcium in the

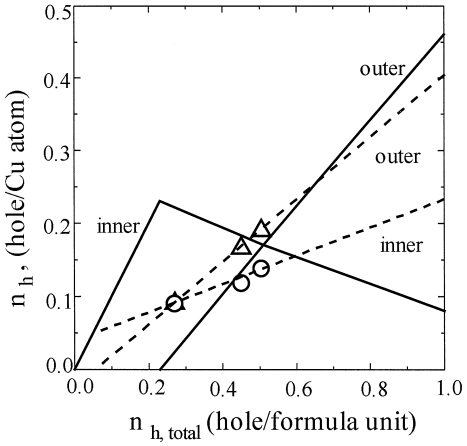

Fig. 9. The concentration of holes in the inner and outer layers of $Tl_2Ba_2Ca_2Cu_3O_{10-\delta}$ as a function of the total number of holes transferred from the TlO layers. The solid lines are the results of calculation in the frame of the point charge model proposed by Haines and Tallon [5]. Dashed lines fit n_h, estimated from the ^{63}Cu NQR data for different CuO_2 layers of Tl2223 with $T_c = 117$ K, $T_c = 104$ K studied in this work and $T_c = 123$ K [16].

Ca layers changing the average charge at the calcium sites and, may be, reducing the concentration of holes in the nearest CuO_2 planes. This additional distribution of charge within layers contributes to the electrostatic energy and should make the magnitude of the real Madelung energy to be different from the value calculated for ideal structure. The dependencies n_h vs. $n_{h,tot} = 2n_h(Cu(1)O_2) + n_h(Cu(2)O_2)$ are drawn at Fig. 9 with dashed lines and these lines are related to the case with adjusted parameter $(m^*/m_e)/e = 0.1$ (see Ref. [5] for details). Unfortunately, $Tl_2Ba_2Ca_2Cu_3O_{10-\delta}$ exist only in a narrow range of δ which do not allow one to study experimentally the strongly underdoped state, where the inequality $n_h(Cu(1)O_2) < n_h(Cu(2)O_2)$ is predicted.

5. Conclusions

The results obtained in this investigation can be summarized as follows.

(1) The different temperature dependence of the uniform spin susceptibility $\chi_s(q = 0)$ for the crystallographically inequivalent CuO_2 layers was revealed for the overdoped sample. A sharper decrease of $\chi_s(T)$ with temperature occurs for the inner layer. This may be considered as due to the lower concentration of hole carriers in this layer in comparison with n_h for the outer layer which is less distant from the acceptor TlO layer.

(2) The difference in the levels of doping for the inequivalent CuO_2 layers disappears in going towards the underdoped state of Tl2223. This is supported by the same temperature dependencies Knight shifts $^{17,63}K$ in different layers CuO_2.

(3) The electric field gradient data were obtained for atoms in inequivalent copper planes and estimates of the hole numbers at Cu and oxygen sites were extracted as well: (i) in the underdoped state of Tl2223 ($T_c = 104$ K) the hole numbers $n_{x^2-y^2}$ and concentration of doped holes δn are close in the inner and outer CuO_2 layers; (ii) when the doping degree increases the quantities $n_{x^2-y^2}$ and δn are increased in each of the CuO_2 layers; (iii) when the total number of holes increases, the difference in δn between inequivalent CuO_2 layers is increased: in outer layer δn(Cu1) is increased faster than δn(Cu2) in inner layer; (iv) the value of $n_{x^2-y^2}/(n_{p\sigma} + n_{p\pi})$ in Tl2223 decreases when increasing the doping degree. This gives evidence that the holes doped into the CuO_2 layers are mainly located in the oxygen orbitals.

(4) It has been pointed out that concentration of the mobile holes in inequivalent CuO_2 planes becomes different in going from the underdoped towards the overdoped $Tl_2Ba_2Ca_2Cu_3O_{10-\delta}$. Inhomogeneity of the distribution of hole carriers increases with doping level of the compound.

Acknowledgements

The work was supported by Russian Scientific Programme Actual Problems of Condensed Matter Physics (subprogram Superconductivity, Project 96 123), Russian State Programme for promotion of the leader scientific schools (Grant 96-15-96515) and by Ministry of Sciences (Programme of International Scientific Cooperation, project 'Radiospectroscopy'). The financial support of International Science Foundation (Grant GR92300) is also gratefully acknowledged.

References

[1] H. Takagi, T. Ido, S. Ishibashi, M. Uota, S. Uchida, Y. Tokura, Phys. Rev. B 40 (1989) 2254.
[2] W.A. Groen, D.M. de Leeuw, L.F. Feiner, Physica C 165 (1990) 55.
[3] M.R. Presland, J.L. Tallon, R.G. Buckley, R.S. Liu, N.E. Flower, Physica C 176 (1991) 95.
[4] M. Di Stasio, K.A. Muller, L. Pietronero, Phys. Rev. Lett. 64 (1990) 2827.
[5] E.M. Haines, J.L. Tallon, Phys. Rev. B 45 (1992) 3127.
[6] H. Alloul, J. Appl. Phys. 69 (1991) 1.
[7] M. Takigawa, A.P. Reyes, P.C. Hammel, J.D. Tompson, R.H. Heffner, Z. Fisk, K.C. Ott, Phys. Rev. B 43 (1991) 247.
[8] N. Winzek, M. Mehring, Appl. Magn. Res. 3 (1992) 422.
[9] A. Trokiner, L.L. Noc, J. Scneck, A.M. Pougnet, R. Mellet, J. Primot, H. Savary, M. Gao, S. Aubry, Phys. Rev. B 44 (1991) 2426.
[10] R. Dupree, Z.P. Han, A.P. Howes, D.M. Paul, M.E. Smith, S. Male, Physica C 169 (1991) 269.
[11] B.W. Statt, L.M. Song, Phys. Rev. B 48 (1993) 3536.
[12] Z.P. Han, R. Dupree, A.P. Howes, R.S. Liu, P.P. Edwards, Physica C 235–240 (1994) 1709.
[13] A.P. Howes, R. Dupree, Z.P. Han, R.S. Liu, P.P. Edwards, Phys. Rev. B 47 (1993) 11529.
[14] Z.P. Han, R. Dupree, R.S. Liu, P.P. Edwards, Physica C 226 (1994) 106.
[15] G.-Q. Zheng, Y. Kitaoka, K. Asayama, K. Hamada, H. Yamauchi, S. Tanaka, Physica C 260 (1996) 197.
[16] A.M. Bogdanovich, K.N. Mikhalev, Y.I. Zhdanov, Y.V. Piskunov, S.V. Verkhovskii, V.V. Lavrentyev, B.A. Aleksashin, A.I. Akimov, A.P. Chernyakova, Supercond.: Phys. Chem. Technol. 6 (1993) 600.
[17] Y.V. Piskunov, K.N. Mikhalev, Y.I. Zhdanov, A.P. Gerashenko, S.V. Verkhovskii, E.Y. Medvedev, A.Y. Yakubovskii, L.D. Shustov, A. Trokiner, Supercond.: Phys. Chem. Technol. 7 (1994) 1193.
[18] Y.I. Zhdanov, K.N. Mihkalev, B.A. Aleksashin, S.V. Verkhovskii, A.M. Bogdanovich, A.I. Akimov, A.P. Chernyakova, Supercond.: Phys. Chem. Technol. 3 (1990) 182.
[19] D.M. Ogborne, M.T. Weller, P.C. Lanchester, Physica C 200 (1992) 167.
[20] S. Kambe, H. Yasuoka, A. Hayashi, Y. Ueda, Technical report of ISSP, Ser. A, No. 2551, 1992.
[21] A. Trokiner, K.M. Mikhalev, A. Yakubovskii, P.-V. Bellot, S. Verkhovskii, Y. Zhdanov, Y. Piskunov, L. Shustov, A. Inyushkin, A. Taldenkov, Physica C 255 (1995) 204.
[22] R.B. Creel, R.G. Barnes, R.J. Schoenberger, R.G. Barnes, D.R. Torgeson, J. Chem. Phys. 60 (1974) 2310.
[23] M. Horvatic, T. Auler, C. Berthier, Y. Berthier, P. Butaud, W.G. Clarc, J.A. Gillet, P. Segransan, J.Y. Henry, Phys. Rev. B 47 (1993) 3461.
[24] C. Berthier, M.H. Julien, M. Horvatic, Y. Berthier, J. Phys. I France 6 (1996) 2205.
[25] A. Trokiner, in: J. Bok, G. Deutscher (Eds.), The Gap Symmetry and Fluctuations In High Temperature Superconductors, Plenum, 1998, in press.
[26] M. Mehring, Appl. Magn. Res. 3 (1992) 383.
[27] K. Hanzawa, J. Phys. Soc. Jpn. 62 (1993) 3302.
[28] A.J. Millis, H. Monien, D. Pines, Phys. Rev. B 42 (1990) 167.
[29] H. Monien, D. Pines, M. Takigawa, Phys. Rev. B 43 (1991) 258.
[30] H. Monien, P. Monthoux, D. Pines, Phys. Rev. B 43 (1991) 275.
[31] H. Monien, D. Pines, C.P. Slichter, Phys. Rev. B 41 (1990) 11120.
[32] K. Schwarz, C. Ambrosch-Draxl, P. Blaha, Phys. Rev. B 42 (1990) 2051.
[33] C. Ambrosch-Draxl, P. Blaha, K. Schwarz, Phys. Rev. B 44 (1991) 5141.
[34] J. Yu, A.J. Freeman, R. Podloucky, P. Herzig, P. Weinberger, Phys. Rev. B 43 (1991) 532.
[35] S. Fraga, J. Karwowik, K.M.S. Saxena, Handbook of Atomic Data, Elsevier, Amsterdam, 1976.
[36] G.-Q. Zheng, Y. Kitaoka, K. Ishida, K. Asayama, J. Phys. Soc. Jpn. 64 (1995) 2524.
[37] Y. Ohta, W. Koshibae, S. Maekawa, J. Phys. Soc. Jpn. 61 (1992) 2198.
[38] R. Stern, M. Mali, I. Mangelschots, J. Roos, D. Brinkmann, J.Y. Genond, T. Graf, J. Muller, Phys. Rev. B 50 (1994) 426.
[39] M.A. Tanatar, V.S. Yefanov, V.V. Dyakin, A.I. Akimov, A.P. Chernyakova, Physica C 185–189 (1991) 1247.
[40] V.T. Adonkin, V.V. Dyakin, V.S. Yefanov, M.A. Tanatar, A.I. Akimov, A.P. Chernyakova, Physica C 185–189 (1991) 1037.